Seismic Hazard Analysis for Southern Slope of the Greater Caucasus (Azerbaijan)

G. Babayev,[1] L. Telesca,[2] S. Agayeva,[1] T. Ismail-zade,[1] I. Muradi,[1] Y. Aliyev,[1] and M. Aliyev[1]

Abstract—In this paper seismic hazard for the southern slope of the Greater Caucasus (Azerbaijan) was assessed by using five major parameters: moment magnitude, simulated peak ground acceleration (PGA) from four target earthquakes, intensity scenario, amplification factor and b value. The deterministic scenario-based seismic hazard assessment method was applied by using the seismic catalogues compiled by the Republican Center of Seismological Survey at Azerbaijan National Academy of Sciences. Additionally this study presents hazard assessment analysis on 67 active faults tracing in the southern slope of the Greater Caucasus, considering the fault's location, size and length, and calculating the magnitude for those faults and lineaments estimated by empirical correlations. Our findings are: (1) maximum earthquake of Mw 8.0 is estimated for the western area zone and is used to generate one of the seismic scenarios of the region; (2) intensity distribution classifies the region into the highest hazard level with intensity value of 7 and over in the westward part and also in the eastward of the studied territory, in contrast to some areas in the southern part of the region which has the lowest level with intensity value of 6 and over; (3) the b value distribution shows that lower values are observed in the western part of the region (Zagatala, Sheki), in the Shamakhi area and on some areas of the northern part indicating higher stress in those areas; (4) PGA map from scenario earthquakes demonstrates that the very high PGAs are scattered in the west and east parts of the study area, while independently from the epicenter of the target earthquakes, the low and very low PGA is scattered in the central part of the study area. Such seismic hazard analysis with consideration of one of the main five parameters and target earthquake scenarios could help the region's sustainable development against earthquakes.

Keywords: Seismic hazard, PGA, b value, intensity, estimated magnitude, Greater Caucasus.

1. Introduction

The study area is the southern slope of the Greater Caucasus (Fig. 1) situated in an intraplate setting within the Eurasian plate and characterized by relatively strong seismicity and focusing on the area with location in 40° 10′ 20.63″/41° 46′ 39.64″ N latitudes and 46° 17′ 15.18″/49° 30′ 13.52″ E longitudes.

The main objective of the paper is to carry out seismic hazard analysis to quantitatively estimate and empirically define the expected hazard in the southern slope of the Greater Caucasus (Azerbaijan). In this study, we perform a strong ground motion simulation for the southern slope of the Greater Caucasus from the integrated analysis of seismicity, geology, effects of soil and rock to seismic wave amplification, attenuation characteristics and site response. Site characterization and identification of the types of sediments, thickness and variations of underlying rock layers was determined by measurement of the P-wave velocities in several boreholes. Shear wave velocity (Vs) was estimated from the empirical relationship with the Vp value. A number of studies concluded that shear wave velocity was an important parameter for evaluating the dynamic behaviour of soil in the near surface depth (Kanli et al. 2006, 2008). Subsurface shear wave velocity values are one of the significant values in calculating seismic hazards (Kanlı 2010). Applying the macroseismic parameters of the target earthquakes and empirical equations, we develop particular earthquake scenarios based on PGA values and consequently hazard level is established considering the spatial distribution of intensity, amplification factor and b values. A seismic hazard map which depicts PGA distribution helps in deciding the location of important and critical objects and other structures. Besides to the

[1] Geology and Geophysics Institute, Azerbaijan National Academy of Sciences, H. Javid Ave 119, AZ1143 Baku, Azerbaijan.
[2] National Research Council, Institute of Methodologies for Environmental Analysis, C. da S. Loja, 85050 Tito, PZ, Italy. E-mail: luciano.telesca@imaa.cnr.it
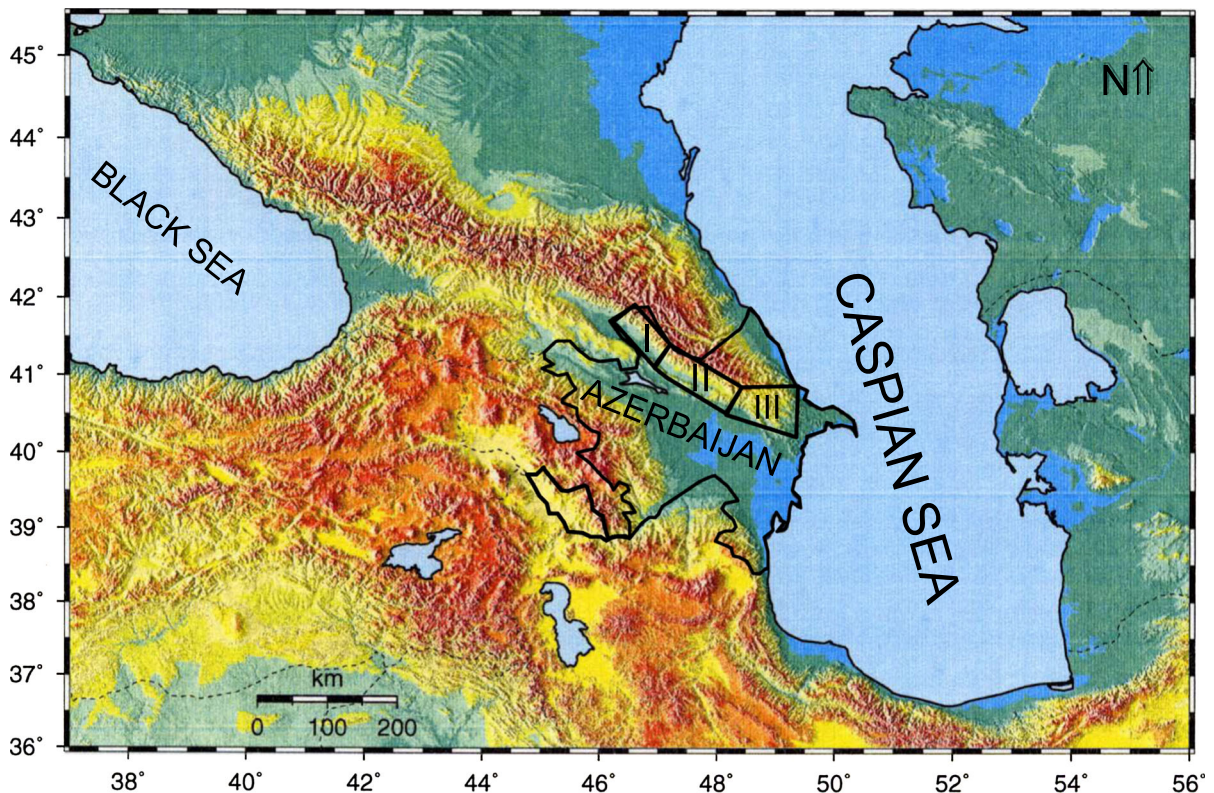
Figure 1
Location map of the study area (I—Balaken–Zagatala, II—Sheki–Oguz–Gabala, III—Ismailli–Shamakhi)

earthquake scenarios, we apply the approach in which the source responsible for the potential hazards in the area is accepted as the causative source representing a maximum seismic "threat" for the area. Here, we perform seismic hazard analysis in terms of maximum magnitude the source (faults and lineaments) can generate using empirical relationship between magnitude and the length of the faults and lineaments.

2. Seismotectonics of the Study Area

As part of the Alpine–Himalayan orogenic belt, Azerbaijan is situated in the active continent collision of the Arabian–Eurasian plates and involved in dynamics of lithospheric structural units of those plates (Jackson et al. 2002). Mountains of the Greater Caucasus extend between the Black and Caspian seas. The Greater Caucasus is wholly situated in an intraplate setting within the Eurasian plate. Southern slope of the Greater Caucasus is characterized by two mountain ranges, with an average elevation of about 4466 m (Alizadeh et al. 2016).

Seismically, the territory of southern slope of the Greater Caucasus is characterized by a high seismic activity (Fig. 2a) (Babayev et al. 2019). Strong and catastrophic earthquakes, which happened several times in this area from ancient times till now caused large number of human losses and destructions. Seismically active block I (Fig. 2a) is located in the north-western part of Azerbaijan Greater Caucasus. This area is shaken both by local focal zones within this block, by Georgian focal zones and by those from Russian part of the Greater Caucasus (Babayev et al. 2019). The historical catalogues registered the local earthquakes in this area since 1853 with intensity of IV–V (Kuliyev 1986; Kondorskaya and Shebalin 1982). The strongest historical Zagatala earthquake occurred in this block in 1936 with intensity of VII
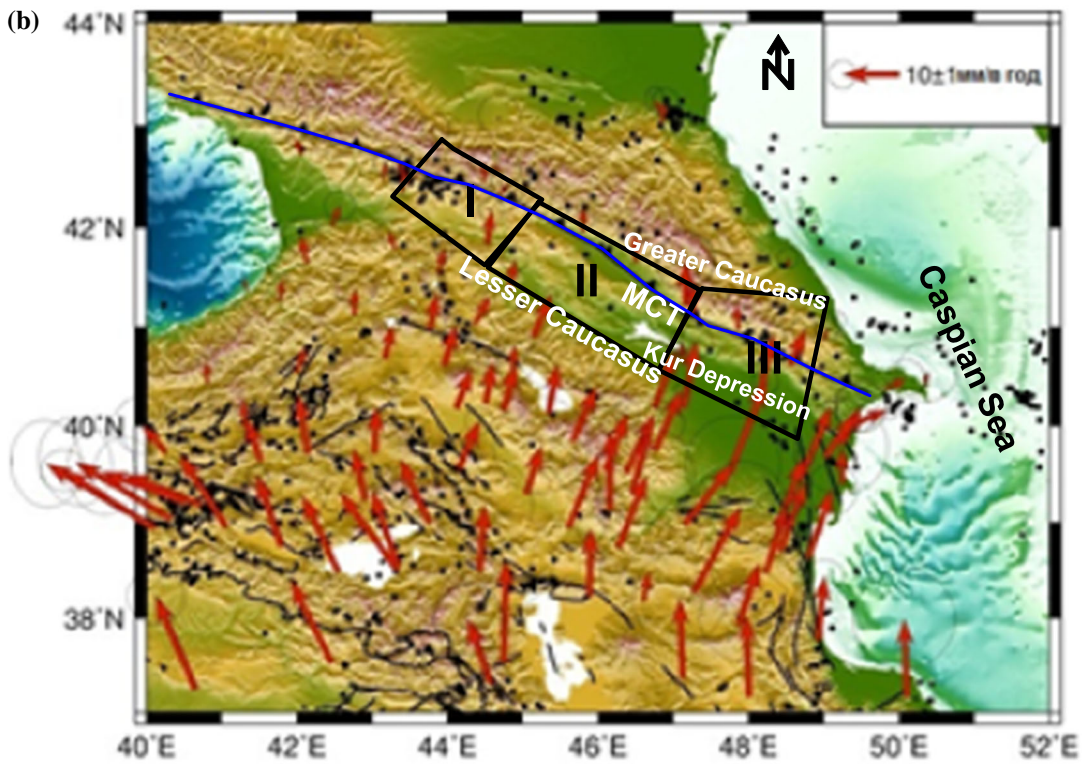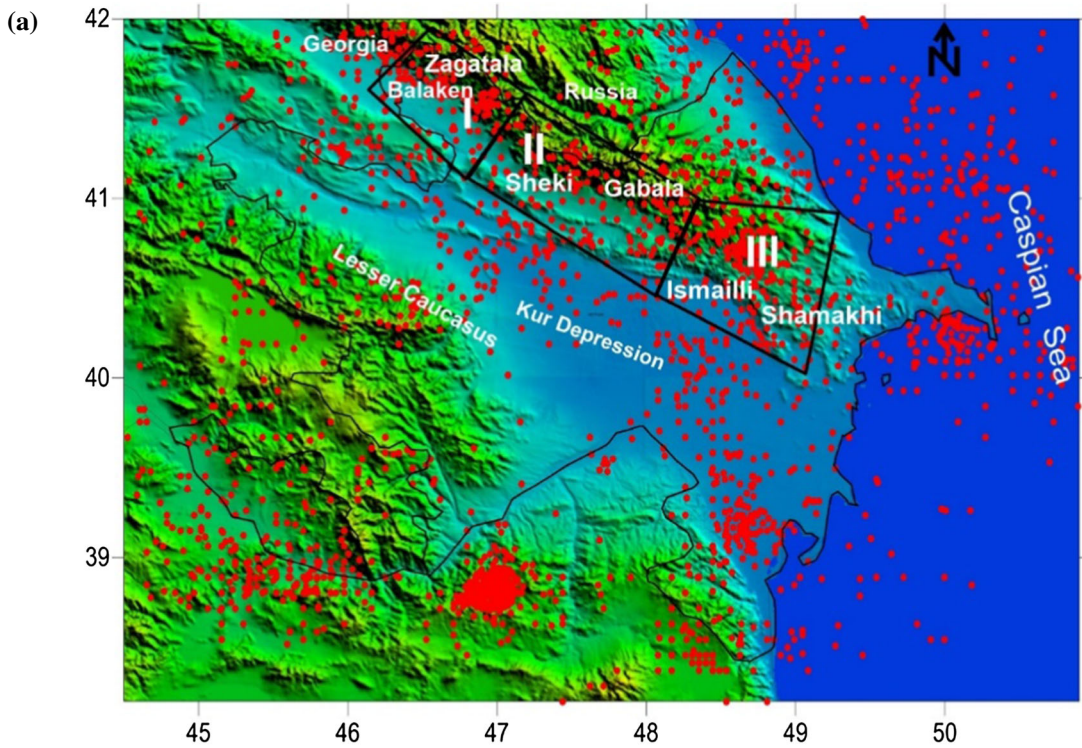
(a)

(b)

(Babayev et al. 2019). Seismically active block II (Fig. 2a) is characterized by the strongest earthquakes which were mainly registered in Sheki and Gabala city areas in 1903, 1928, 1953, 1963 years with intensity of VII. Prior to 1828 year, there occurred 35 earthquakes with weak seismic effect (Babayev et al. 2019). The strongest earthquakes which are framed by block III (Fig. 2a) mainly occurred in Shamakhi and Ismailli city areas (Babayev 2010; Babayev et al. 2010; Babayev and Telesca 2014; Kadirov et al. 2012, 2013; Telesca et al. 2013, 2017; Yetirmishli et al. 2013). The city of Shamakhi (situated about 110 km westward from capital of Azerbaijan, Baku city) was struck by strong seismic events in the past: in 1191, 1667, 1859 and 1902 (Veber 1904; Kondorskaya et al. 1982). Some of them have the magnitude of 6.0–6.9. Those earthquakes were felt in the epicenter with the intensity IX (according to the MSK-64 scale). Some earthquakes with M ~ 5.0 also occurred in this region with intensity in the epicenter at VII (MSK-64).

Within contemporary period between 2000 and 2018, the most felt earthquakes occurred in 2012 in Sheki–Gabala zone, in 2015 in Sheki–Oguz zone, in 2016 and 2018 in Zagatala zone with local magnitude M = 4.5 ~ 5.5. The strongest one occurred in 2014, 2016, 2019 in Shamakhi–Ismailli zone with local magnitude M = 6.0–6.9.

The GPS data indicates that total convergence across the central and western Lesser Caucasus and Greater Caucasus is ~ 10 ± 2 mm/year (McClusky et al. 2000). Repeating GPS measurements in Azerbaijan show active convergence between the Lesser Caucasus/Kur Depression and the Greater Caucasus with strain concentrated along Main Caucasus Thrust (MCT, blue line in Fig. 2b) (Philip et al. 1989; Reilinger et al. 2006; Kadirov 2000; Kadirov et al. 2012; Telesca et al. 2017). The Balaken–Zagatala zone and the Ismailli–Shamakhi zone are characterized by the

extension, giving rise to mainly normal dip slips and normal dip slips with strike slip motion (Babayev et al. 2017; Agayeva et al. 2009). Sheki–Gabala zone is mostly compression with the thrust and reverse faults (Kadirov et al. 2013).

3. Materials and Methods

3.1. Basemap and Meshing the Study Area

Using the geological map of Azerbaijan (Alizadeh 2008; Alizadeh et al. 2016) as a basemap, the study area with blocks [I, II and III, respectively (see Fig. 2)] was framed considering specific geological features (Khalilov et al. 1987), tectonic peculiarities (Kangarli and Akhundov 1998; Khain et al. 2005), and then was meshed into 46 cells with a step of 10×10 km^2 (Fig. 3).

Geologically, the area is represented by Quaternary system (Holocene and Pleistocene), Neogene and Paleogene of Cenozoic, Cretaceous and Jurassic systems of Mesozoic (Alizadeh 2008). The lithology of the study area consists mainly of argillites, limestone, marlstone, sandstone, dolomites, aleurolite and clayey shales. Lithological factor is one of the important steps in seismic hazard assessment and is a necessary parameter in deterministic seismic hazard analysis (Babayev et al. 2010; Babayev and Telesca 2016). We will come back to that factor below in the respective section of the present paper.

3.2. Average Earthquake Magnitude Estimated for Various Sources

To assess the moderate maximum magnitude potential of the various faults and lineaments tracing in the study region empirical formulas of Shebalin (1961), Gubin (1974), Riznichenko (1965), Utsi (1961), Mammadli (2007), Bonilla et al. (1984) were applied (Fig. 4). The Scordilis' formula (2006) was applied to convert the magnitudes to moment magnitude Mw in the equations of Shebalin (1961), Gubin (1974), Riznichenko (1965), Utsi (1961), Mammadli (2007) and Bonilla et al. (1984).

The length of each fault and lineament was calculated by applying ArcGIS 10.0 (ESRI 2011)
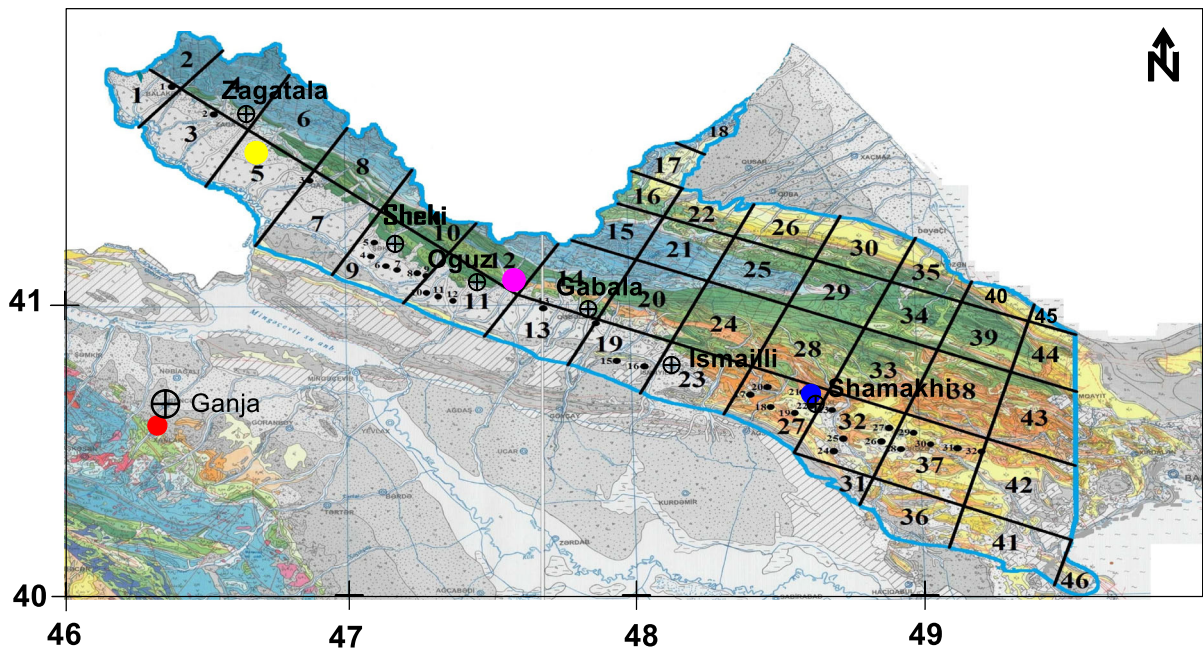
Figure 3
Basemap and meshing the study area (scale 1:500,000). Target earthquakes for this study are demonstrated by circle of respective colors. See text for detail below

software. The rupture length of the faults and lineaments was taken as one-third of the fault length according to (Baghbani et al. 2016). Totally, in the study area there were 67 fault and lineament parts. The length of the faults and lineaments in the study zone, the estimated magnitude based on empirical relations are shown in Table 1.

It is observed that the estimated maximum magnitude of 8.0 is spread in the western area zone and is used to generate one of the seismic scenarios of the region (Fig. 5).

3.3. Earthquake Scenario. PGA Distribution

Four target earthquakes for PGA and intensity scenarios were considered: M = 6.8 Ganja earthquake occurred in 1139 with focal depth (h) of 15 km as near-field event (Fig. 3, marked in red color), M = 6.8 Shamakhi earthquake occurred in 1902 with h = 15 km as local-field event (Fig. 3, marked in blue), M = 5.9 Sheki–Oguz earthquake occurred in 2015 with h = 13 km as local-field event (Fig. 3, marked in pink) and M = 5.5 Zagatala earthquake

occurred in 2018 with h = 10 km as local-field event (Fig. 3, marked in yellow). The selection of the target earthquakes was based on the distance from the study area (Ganja earthquake) and various epicenters in the study area (the rest target earthquakes), their magnitude, their effect on the study area, their location with respect to the regional fault system (Babayev et al. 2010; Babayev and Telesca 2016).

Macroseismic parameters (magnitude, focal depth, epicentral/hypocentral distances to each cell of the study area) of above-mentioned four target events were used in modelling ground motion for each cell at bedrock and surface level (Babayev et al. 2010). The expected bedrock PGA was estimated with Eq. (1) that is the relation between the peak ground acceleration A (in gal) (in gal = 10^{-2} m s^{-2}), the magnitude M, and the hypocentral distance R (in km):

$$\log A = 0.28M - 0.8\log R + 1.7 \qquad (1)$$

for $A > 160$ gal (for local and near-field events).

Derived empirically by Aptikayev and Kopnichev (1979), the Eq. (1) is well suited for soft to hard bedrocks, typical for the bedrocks in Azerbaijan. A
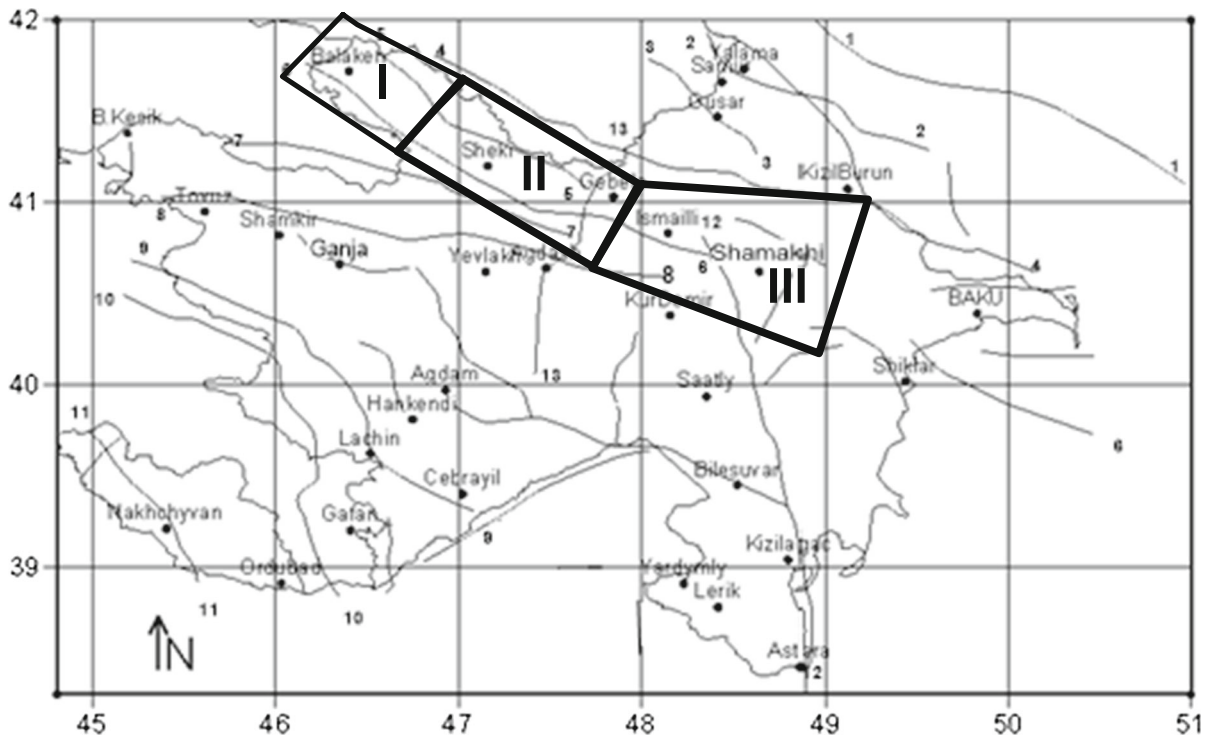
Figure 4
Fault map of the study area. Some faults are compiled from geologic maps and divided into thrusts and remaining fault types. Some faults are interpreted from gravity data (from Kadirov 2000; Nemčok et al. 2011). Faults: 1-1 Makhachkala-Krasnovodsk, 2-2 Akhty-Nyugedi-Kiliazin, 3-3 Siyazan, 4-4 Zangi-Kozluchay, 5-5 Vandam, 6-6 Alazan-Agrichay-Alat, 7-7 Kur, 8-8 Pre-Caucasus, 9-9 Bashlybelsky, 10-10 Gektana-Akerinskiy, 11-11 Sharur-Ordubad, 12-12 Gizilagach, 13-13 Arpa-Samur

horizontally multi-layered structure, where shear-wave velocity, thickness, and density depend on the layers, is used to model the subsurface structure down to the seismic bedrock (Babayev et al. 2010; Babayev and Telesca 2016). The subsurface ground model for each cell and the identification of the types of sediments, their thickness and variations of underlying rock layers was developed by means of the measurement of the P-wave velocities in several boreholes (Babayev and Telesca 2014). P-wave velocity test was performed in the laboratory, on-site and on the samples retrieved from the boreholes (Kangarli and Akhundov 1998). Rock blocks were collected from various stone quarries located around Shamakhi, Sheki, Oguz, Gabala. Each rock block was inspected in order to guarantee that it would provide standard testing specimens without macroscopic defects, alteration zones and fractures (Babayev and Telesca 2014, 2016). Vp is measured on samples by

direct transmission using ultrasonic nondestructive tester that measures the time of propagation of ultrasound pulses (Babayev and Telesca 2016). The subsurface models used in our study are presented in Table 2. Shear wave velocity V_S (m s^{-1}) averaged over top 30 m of the soil are estimated from empirical relationship with the V_p value in Eq. (2). In its turn, V_p value was measured for the specific soils by experimental method (Seed et al. 1969).

$$V_S = V_P/(4.34 - 0.49V_P) \qquad (2)$$

For hard sedimentary rocks, the amplification factor within a layer has been calculated by using the Eq. (3) (Midorikawa et al. 1992):

$$\log A_{PGA} = 1.11 - 0.42 \log V_S \qquad (3)$$

where A_{PGA} is the amplification factor of peak ground acceleration between target layer and the layer with $V_s = 440$ m/s. Shear wave velocity (Vs)

Table 1

Magnitude calculations for various faults and lineaments (Fig. 4) estimated by empirical correlations

No.	L (km)	Shebalin (1961)	Gubin (1974)	Riznichenko (1965)	Utsi (1961)	Mammadli (2007)	Bonilla et al. (1984)	Av (Mw)
1	30	5.0	6.5	6.5	6.6	6.4	7.1	6.3
2	35	5.1	6.7	6.6	6.7	6.6	7.1	6.5
3	88	5.9	7.6	7.1	7.5	7.7	7.4	7.2
4	13	4.2	5.7	6.1	5.8	5.5	6.8	5.7
5	22	4.7	6.2	6.4	6.3	6.1	7.0	6.1
6	35	5.1	6.7	6.6	6.7	6.6	7.1	6.5
7	17	4.5	5.9	6.2	6.1	5.8	6.9	5.9
8	19	4.6	6.1	6.3	6.2	5.9	6.9	6.0
9	34	5.1	6.7	6.6	6.7	6.6	7.1	6.4
10	11	4.1	5.5	6.0	5.7	5.3	6.8	5.5
11	22	4.7	6.2	6.4	6.3	6.1	7.0	6.1
12	18	4.5	6.0	6.2	6.1	5.8	6.9	5.9
13	23	4.7	6.3	6.4	6.3	6.1	7.0	6.1
14	7	3.7	5.0	5.7	5.3	4.7	6.6	5.2
15	20	4.6	6.1	6.3	6.2	6.0	7.0	6.0
16	22	4.7	6.2	6.4	6.3	6.1	7.0	6.1
17	20	4.6	6.1	6.3	6.2	6.0	7.0	6.0
18	20	4.6	6.1	6.3	6.2	6.0	7.0	6.0
19	35	5.1	6.7	6.6	6.7	6.6	7.1	6.5
20	10	4.0	5.4	5.9	5.6	5.1	6.7	5.5
21	15	4.4	5.8	6.1	6.0	5.6	6.9	5.8
22	20	4.6	6.1	6.3	6.2	6.0	7.0	6.0
23	30	5.0	6.5	6.5	6.6	6.4	7.1	6.3
24	40	5.2	6.8	6.7	6.8	6.8	7.2	6.6
25	11	4.1	5.5	6.0	5.7	5.3	6.8	5.5
26	23	4.7	6.3	6.4	6.3	6.1	7.0	6.1
27	8	3.8	5.2	5.8	5.4	4.9	6.7	5.3
28	5	3.4	4.7	5.5	5.0	4.3	6.5	4.9
29	6	3.6	4.9	5.6	5.2	4.5	6.6	5.1
30	35	5.1	6.7	6.6	6.7	6.6	7.1	6.5
31	5	3.4	4.7	5.5	5.0	4.3	6.5	4.9
32	40	5.2	6.8	6.7	6.8	6.8	7.2	6.6
33	20	4.6	6.1	6.3	6.2	6.0	7.0	6.0
34	20	4.6	6.1	6.3	6.2	6.0	7.0	6.0
35	40	5.2	6.8	6.7	6.8	6.8	7.2	6.6
36	35	5.1	6.7	6.6	6.7	6.6	7.1	6.5
37	20	4.6	6.1	6.3	6.2	6.0	7.0	6.0
38	10	4.0	5.4	5.9	5.6	5.1	6.7	5.5
39	8	3.8	5.2	5.8	5.4	4.9	6.7	5.3
40	18	4.5	6.0	6.2	6.1	5.8	6.9	5.9
41	30	5.0	6.5	6.5	6.6	6.4	7.1	6.3
42	20	4.6	6.1	6.3	6.2	6.0	7.0	6.0
43	27	4.9	6.4	6.5	6.5	6.3	7.1	6.3
44	20	4.6	6.1	6.3	6.2	6.0	7.0	6.0
45	20	4.6	6.1	6.3	6.2	6.0	7.0	6.0
46	14	4.3	5.7	6.1	5.9	5.5	6.9	5.7
47	200	6.6	8.5	7.6	8.2	8.7	7.7	7.9
48	30	5.0	6.5	6.5	6.6	6.4	7.1	6.3
49	36	5.1	6.7	6.6	6.7	6.7	7.1	6.5
50	7	3.7	5.0	5.7	5.3	4.7	6.6	5.2
51	46	5.3	7.0	6.8	6.9	6.9	7.2	6.7
52	37	5.1	6.7	6.6	6.7	6.7	7.2	6.5
53	85	5.9	7.6	7.1	7.5	7.7	7.4	7.2
54	70	5.7	7.4	7.0	7.3	7.4	7.3	7.0
55	8	3.8	5.2	5.8	5.4	4.9	6.7	5.3

Table 1 *continued*

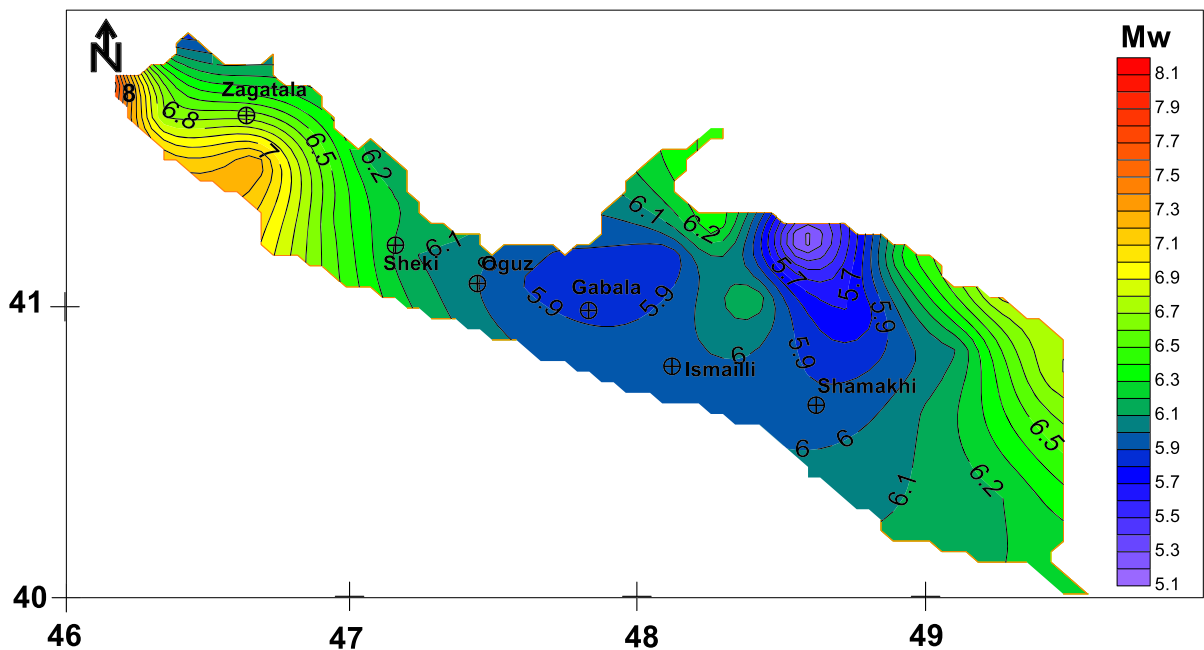| No.	L (km)	Shebalin (1961)	Gubin (1974)	Riznichenko (1965)	Utsi (1961)	Mammadli (2007)	Bonilla et al. (1984)	Av (Mw)
56	40	5.2	6.8	6.7	6.8	6.8	7.2	6.6
57	50	5.4	7.0	6.8	7.0	7.0	7.2	6.8
58	65	5.6	7.3	7.0	7.2	7.4	7.3	7.0
59	38	5.2	6.8	6.7	6.8	6.7	7.2	6.5
60	8	3.8	5.2	5.8	5.4	4.9	6.7	5.3
61	10	4.0	5.4	5.9	5.6	5.1	6.7	5.5
62	14	4.3	5.7	6.1	5.9	5.5	6.9	5.7
63	22	4.7	6.2	6.4	6.3	6.1	7.0	6.1
64	16	4.4	5.9	6.2	6.0	5.7	6.9	5.8
65	58	5.5	7.2	6.9	7.1	7.2	7.3	6.9
66	10	4	5.4	5.9	5.6	5.1	6.7	5.5
67	30	5.0	6.5	6.5	6.6	6.4	7.1	6.3

Figure 5
Moment magnitude Mw based for various faults and lineaments

has the advantages of reflecting the stiffness of soils (Babayev and Telesca 2014, 2016).

Consequently, Vs is an important parameter in subsoil exploration (Babayev and Telesca 2016). Shear wave velocity (Vs) by itself is a useful parameter for seismic classification of soils (Babayev and Telesca 2016). The reference site condition for which the current research is done equals to 440 m/s which is represented by hard rock (Dobry et al. 2000), typical in the study area. For soft sedimentary rocks

and soils, the amplification factor in a subsurface layer were estimated from shear-wave velocities, density, and thickness of the layer using the SHAKE (Ordónez 2003). The measured and calculated seismic wave velocities, density value, calculated amplification factor for the principal site units used in the ground modelling are demonstrated in Table 2.

Each layer is homogeneous and isotropic with characteristic values of thickness, mass density, shear modulus and damping factor (Babayev and Telesca

Table 2

Lithology and physical parameters of ground units for the study area

| Age	Lithology	Vp (km/s)	Vs (km/s)	Density (kg/sm^3)	Amplification factor
Cenozoic Holocene (modern deposits)	Argillites, limestone, marlstone, sandstone	1.50	0.35	1.9	1.10
Cenozoic, Quaternary, Upper Pleistocene	Thin-layered sandstone	3.30	2.02	2.35	0.53
Cenozoic, Quaternary, Lower Pleistocene	Argillites and sandstone	2.10	0.50	2.00	0.95
Cenozoic, Neogene	Dolomite, marlstone, sandstone	2.67	0.88	1.98	0.75
Cenozoic, Paleogene	Limestone, aleurolite, marlstone	2.23	0.69	1.87	0.83
Mesozoic, Cretaceous	Sandstone, aleurolite and clayey shales	3.93	1.63	2.38	0.58
Mesozoic, Jurassic	Aleurolite, marlstone	4.18	1.82	2.49	0.55
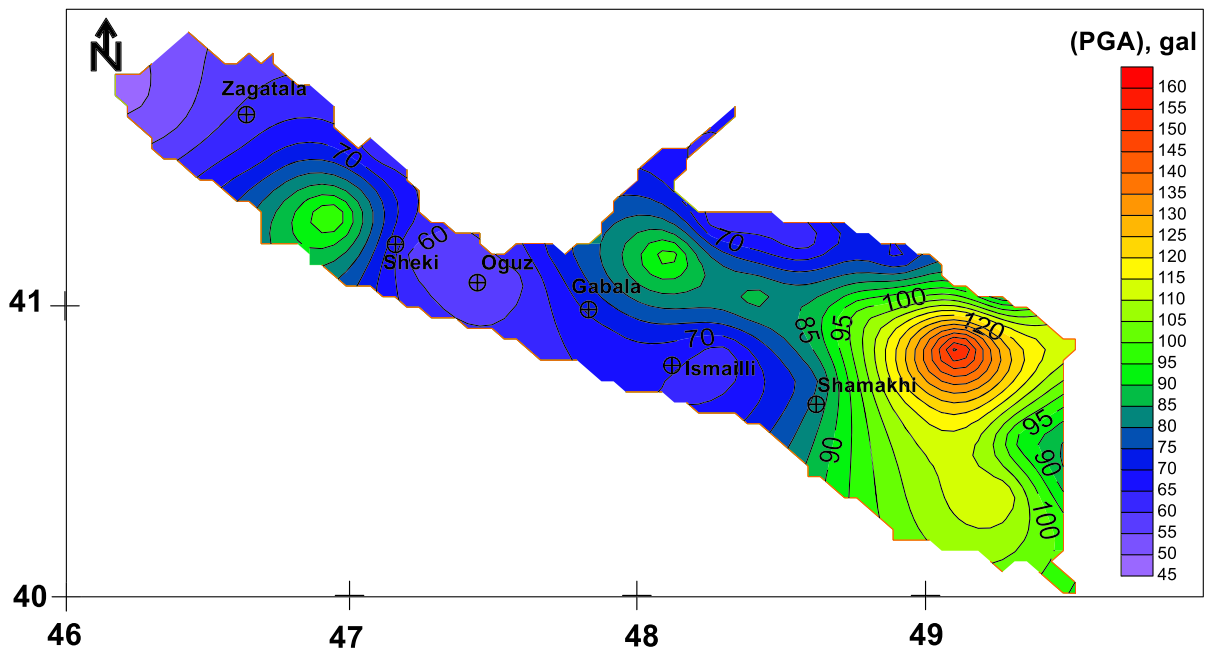
Figure 6
Generalized PGA index map of the study area based on PGAs of four target earthquakes

2016). Since the analysis takes into account the non-linearity of the soils using an iterative procedure, an important role is played by dynamic soil properties (Babayev and Telesca 2016).

The assumptions of the SHAKE method are: (1) the soil system extends infinitely horizontally; (2) the soil responses are due to the upward propagation of shear waves from the underlying rock stratum. Nonlinear site effects, like increasing damping and decreasing shear wave velocity with the increase of input strength, are observed in the dynamic loading of soils (Idriss and Seed 1968).

The amplification function at a site is controlled by the wave velocity and damping in the soil layer hence nonlinear site effects can be expected in strong-motion seismology (Panza et al. 2001, 2011). With the extrapolation of parameters of the target earthquakes, peak ground accelerations for scenario earthquakes were calculated at the magnitudes of selected earthquakes. In conclusion, PGA values from four target earthquakes considering amplification factors for soft rocks derived from SHAKE2000 and for hard rocks derived from Eq. (3) are used to prepare the generalized PGA index map at surface
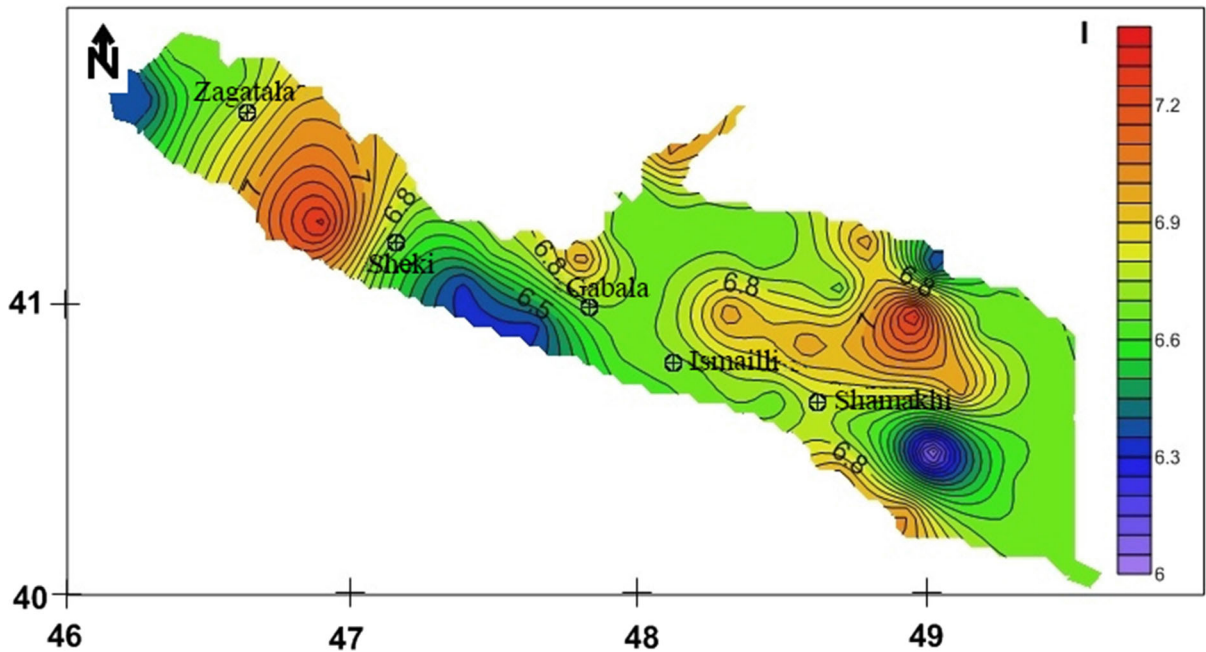
Figure 7
Intensity distribution map for the study area using existing correlation relationship between peak ground acceleration and intensity MSK-64
(Murphy and O'brien 1977; Trifunac and Brady 1975)

level for the study area. The generalized predicted surface PGA derived from the parameters of the target earthquakes and intensity level are plotted in Figs. 6 and 7, respectively. The plotted models show the level of ground shaking over the study area and identify regularities in the attenuation of intensities (Babayev and Telesca 2014). The very high PGA is distributed in the north-eastern part of the study area. Between western part with the very low PGA of 45–50 gal and central part of the study area in Oguz city with the PGA of 60 gal, there is a zone with increasing PGA up to about 100 gal.

Figure 8 shows the amplification factor distribution map of the study area based on the amplification factor values of Table 2. The very high amplification factor was observed in the south-eastern part of the area, while between low value of amplification factor in the western and middle parts, there is increasing spot of amplification factor: this is due to the increasing soft soils, namely soft-cemented sandstone–clay deposits. Such pattern is also scattered in the north and north-eastern parts.

3.4. b value

The b value is one of the important components in the Gutenberg–Richter empirical relation $\log_{10}(N) = a - bM$ (Gutenberg and Richter 1944, 1956). This relation represents the frequency of occurrence of seismic events as a function of their magnitude. The a value describes the seismic productivity, while the b value measures the proportion of number of weak to strong events and indicates the dynamics of the tectonic stress of an area.

Telesca et al. (2017) showed that the seismicity of Azerbaijan from 2003 to 2016 was characterized by a bimodal non-cumulative frequency–magnitude distribution that indicates that seismicity is quite spatially heterogeneous, thus affecting the estimation of the completeness magnitude. Through the Aki's (1965) formula, the b value of the Gutenberg–Richter law can be calculated as (4):

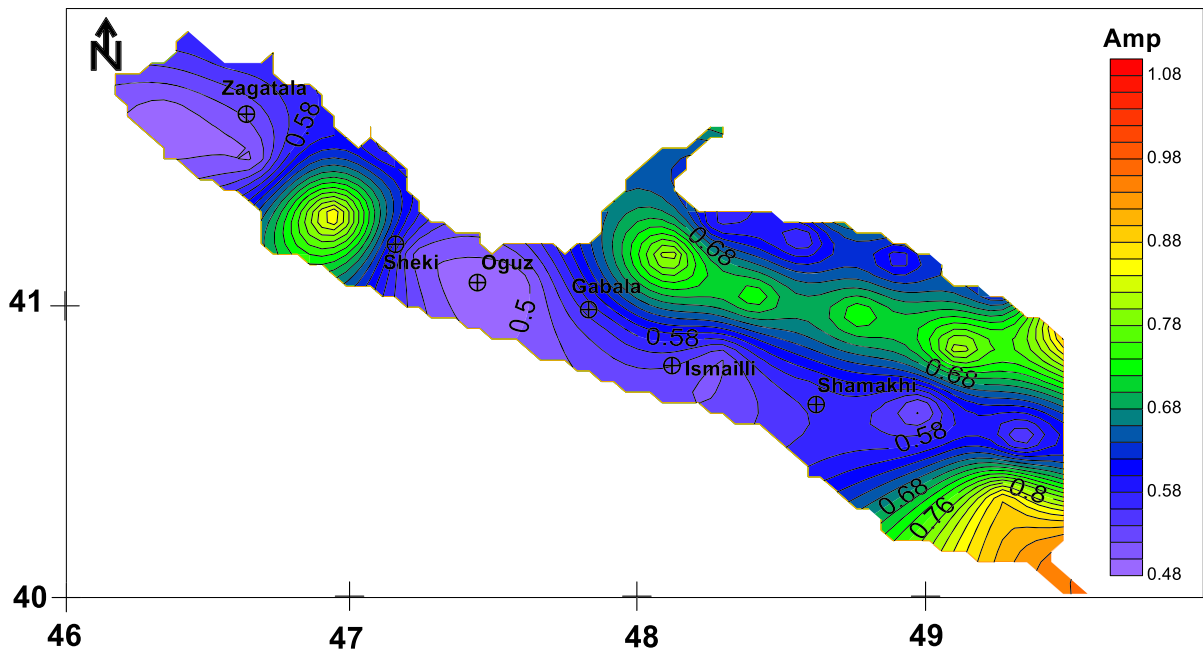$$b = \frac{\log_{10}(e)}{\langle M \rangle - \left(M_c - \frac{\Delta M_{bin}}{2} \right)} \qquad (4)$$

Figure 8
Spatial distribution of amplification factor through study area

where $\langle M \rangle$ is the mean magnitude of the seismic dataset, Mc is the completeness magnitude and ΔMbin is the bin size of the non-cumulative frequency–magnitude distribution.

Thus, as it is clearly seen from the formula above, the estimation of b value depends on that of the completeness magnitude. By using several methods (Wiemer and Wyss 2000). Telesca et al. (2017) found that the more conservative choice of completeness magnitude of the area under study was 2.9. Therefore, in this study we calculated the spatial variation of the b value, considering only the events with magnitude larger or equal to 2.9.

Figure 9 shows the spatial variation of the b value through the region. The lowest b value was estimated in southeast and west which have relatively the highest seismic activity in the studied region.

4. Discussion and Conclusion

In the present study, we applied three main methodological approaches. First, estimation of

potential magnitude that each fault and lineament might produce considering rupture zone (focus of earthquake). Second, development of strong motion model in the values of peak ground acceleration on the basis of the deterministic (scenario-based) seismic hazard assessment approach (DSHA), and third, Gutenberg–Richter relation which is empirical relation in seismology, representing the frequency magnitude distribution considering b value in that equation. The ground acceleration due to strong ground motion depends on an integrated combination of the magnitude, duration, frequency content, hypocentral distance, site effect and site response.

Based on the analysis of seismic hazard with the methods applied in the present study, the southern slope of Greater Caucasus of Azerbaijan represents moderate to high seismic hazard. Estimated maximum magnitude potential of the various faults and lineaments tracing in the study region are observed in the western, eastern zones and some small part of north which have relatively highest risk score among the others. Increasing intensity is observed in the areas with soft-cemented sandstone–clay deposits,
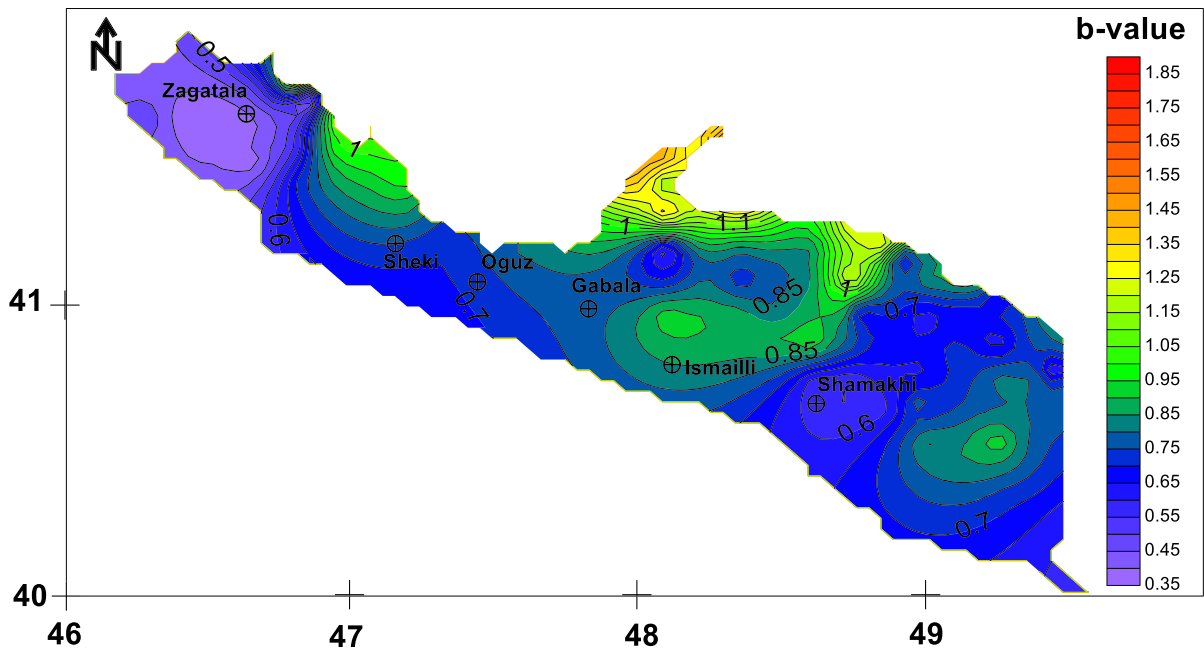
Figure 9
Detailed distribution of Gutenberg–Richter b value in the study area

although in those area there are inclinations of sandstone, limestone and sandy marl of various thicknesses. Such areas are in the western part (Za-gatala–Sheki), in the northern part (Ismailli–Shamakhi) and eastern part of the studied region. Those zones are also characterized by high amplifi-cation factor compared to other zones of the studied region. Amplification factor varies in the range of 0.88–1.00, taking the highest values in the western and eastern zones. The most important fact here is a decrease of amplification factor down to 0.48 between western and eastern (mainly in the center) parts, while simultaneously an increase up to 0.78 scattering in the form of stripe in the northern part. The very high PGA is distributed in the north-eastern part of the study area. Among high values of PGA, there are areas with sharp decrease of PGA, which is most probably interlinked with damping factor of the ground. Intensity map demonstrates that ground dis-placements are various and not obviously oriented towards seismic source. The lowest b value was clearly observed in west and southeast, where large earthquakes occurred in Zagatala and Ismailli–Sha-makhi areas.

Publisher's Note Springer Nature remains neutral with regard to jurisdictional claims in published maps and institutional affiliations.

REFERENCES

Agayeva, S. T., & Babayev, G. R. (2009). Analysis of earthquake focal mechanisms for Greater and Lesser Caucasus applying the method of World Stress Map. Azerbaijan National Academy of

Sciences. In *Proceedings of Geology Institute*, Baku, "Nafta-Press no. 2, Baku, pp. 40–44.

Aki, K. (1965). Maximum likelihood estimate of b in the formula log(N) = a-bM and its confidence limits. *Bulletin of the Earthquake Research Institute University of Tokyo, 43,* 237–239.

Alizadeh, A. A. (Eds). (2008). Geological map of Azerbaijan Republic, Scale 1:500,000, with Explanatory Notes. Baki Kartoqrafiya Fabriki.

Alizadeh, A. A., Guliyev, I. S., Kadirov, F. A., & Eppelbaum, L. V. (2016). *Geosciences of Azerbaijan. Volume I: Geology, 2016* (p. 340). Cham: Springer. https://doi.org/10.1007/978-3-319-27395-2.239.

Aptikayev, F., & Kopnichev, Y. (1979). Considering focal earthquake mechanism at the prediction of strong motion parameters. In *Doklady/Transactions of the U.S.S.R. Academy of Sciences*, vol. 247, pp. 822–825 **(in Russian)**.

Babayev, G. (2010). About some aspects of probabilistic seismic hazard assessment of Absheron peninsula. Republican Seismic Survey Center of Azerbaijan National Academy of Sciences. Catalogue of Seismoprognosis Research Carried Out in Azerbaijan Territory in 2009, "Teknur", Baku, pp. 59–64 **(in Russian)**.

Babayev, G. R., Agayeva, S. T., Ismail-Zade, T. T., Muradi, I. B., & Aliyev, Y. N. (2019). Seismic effect assessment of the southern slope of Greater Caucasus (Azerbaijan) based on the earthquake scenarios: Ground parameters and acceleration models. *Geophysical Journal, 3*(41), 152–170. https://doi.org/10.24028/gzh.0203-3100.v41i3.2019.172471.   **(original in Russian)**.

Babayev, G. R., Akhmedova, E. V., & Kadirov, F. A. (2017). Analysis of stress-strain state of Caucasus region (Azerbaijan) on the basis of maximum horizontal stress vectors and World Stress Map. Application technique. *Geophysical Journal, 3*(39), 26–39. https://doi.org/10.24028/gzh.0203-3100.v39i3.2017.104026.   **(in Russian)**.

Babayev, G., Ismail-Zadeh, A., & Le Mouël, J.-L. (2010). Scenario-based earthquake hazard and risk assessment for Baku (Azerbaijan). *Natural Hazards Earth System Science, 10,* 2697–2712. https://doi.org/10.5194/nhess-10-2697-2010.

Babayev, G., & Telesca, L. (2014). Strong motion scenario of 25th November 2000 earthquake for Absheron peninsula (Azerbaijan). *Natural Hazards, 73*(2014), 1647–1661.

Babayev, G., & Telesca, L. (2016). Site specific ground motion modeling and seismic response analysis for microzonation of Baku, Azerbaijan. *Acta Geophysica, 64*(6), 2151–2170. https://doi.org/10.1515/acgeo-2016-0105.

Baghbani, M., Gholami, E., & Barani, H. R. R. (2016). Probabilistic seismic hazard analysis for a Dam Siyaho in South Khorasan province (Eastern Iran). *Geodynamics Research International Bulletin, 4*(02), 34–48.

Bonilla, M. G., Mark, R. K., & Lienkaemper, J. J. (1984). Statistical relations among earthquake magnitude, surface rupture length and surface fault displacement. *Bulletin of Seismology Society of American, 74,* 2379–2411.

Dobry, R., Borcherdt, R. D., Crouse, C. B., Idriss, I. M., Joyner, W. B., Martin, G. R., et al. (2000). New site coefficients and site classification system used in recent building seismic code provisions. *Earthquake Spectra, 16*(1), 41–67.

ESRI. (2011). *ArcGIS Desktop: Release 10. Environmental Systems Research Institute (ESRI)*. Redlands: ESRI.

Gubin, I. E. (1974). Seismogenic faults and their meaning for seismic zoning. *Geotectonics, 6,* 29–40. **(in Russian)**.

Gutenberg, B., & Richter, C. F. (1944). Frequency of earthquakes in California. *Bulletin of Seismology Society American, 34,* 185–188.

Gutenberg, B., & Richter, C. F. (1956). Magnitude and energy of earthquake. *Annual Geofisiks (Rome), 9,* 1–15.

Idriss, I. M., & Seed, H. B. (1968). Seismic response of horizontal soil layer. *Journal of the Soil Mechanics and Foundations Division ASCE, 94,* 1003–1031.

Jackson, J., Priestley, K., Allen, M., & Berberian, M. (2002). Active tectonics of the South Caspian Basin. *Geophysical Journal International, 148,* 214–245.

Kadirov, F. A. (2000). *Gravity field and models of deep structure of Azerbaijan* (p. 112). Baku: Nafta-Press. **(monograph in Russian)**.

Kadirov, F. A., Floyd, M. A., Alizadeh, A., Guliev, I., Reilinger, R. E., Kuleli, S., et al. (2012). Kinematics of the Caucasus near Baku, Azerbaijan. *Journal of Natural Hazards, 63,* 997–1006. https://doi.org/10.1007/s11069-012-0199-0.

Kadirov, F. A., Gadirov, A. G., Babayev, G. R., Agayeva, S. T., Mammadov, S. K., Garagezova, N. R., et al. (2013). Seismic Zoning of the Southern Slope of Greater Caucasus from the fractal parameters of the earthquakes, stress state and GPS velocities, Izvestiya. *Physics of the Solid Earth, 49*(4), 554–562.

Kangarli, T. N., & Akhundov, A. B. (1998). Surface and deep structure of southern slope of the Greater Caucasus. *Soviet Geology, 10,* 42–52. **(in Russian)**.

Kanlı, A. I. (2010). Integrated approach for surface wave analysis from near-surface to bedrock, Chapter 29, advances in near-surface seismology and ground-penetrating radar, geophysical, pp. 461–476.

Kanli, A. I., Kang, T. S., Pınar, A., Tildy, P., & Pronay, Z. (2008). A systematic geophysical approach for site response of the Dinar Region, South Western Turkey. *Journal of Earthquake Engineering, 12*(1), 165–174.

Kanli, A. I., Tildy, P., Pronay, Z., Pınar, A., & Hermann, L. (2006). V_S30 mapping and soil classification for seismic site effect evaluation in Dinar Region, SW Turkey. *Geophysical Journal International, 165*(1), 223–235.

Khain, V. E., & Alizade, A. A. (2005). *Geology of Azerbaijan. Volume IV. Tectonics* (pp. 214–234). Baku: Nafta-Press. **(in Russian)**.

Khalilov, E., Mekhtiyev, S., & Khain, Y. (1987). Some geophysical data confirming the collisional origin of the Greater Caucasus. *Geotectonics, 21,* 132–136.

Kondorskaya, N., & Shebalin, N. (1982). *New catalog of strong earthquakes in the USSR from ancient times through 1977.* Boulder: World Data Center A for Solid Earth Geophysics.

McClusky, S., Balassanian, S., Barka, A., Demir, C., Ergintav, S., Georgiev, I., et al. (2000). Global positioning system constraints on plate kinematics and dynamics in the eastern Mediterranean and Caucasus. *Journal of Geophysical Research, 105,* 5695–5719. https://doi.org/10.1029/1999jb900351.

Midorikawa, S., Matsuoka, M., & Sakugawa, K. (1992). Evaluation of site effects on peak ground acceleration and velocity observed during the 1987 Chiba-ken-toho-oki earthquake. *Journal of Structural and Construction Engineering Architectural Institute of Japan, 442,* 71–78. **(in Japanese with English abstract)**.

Murphy, J., & O'brien, L. (1977). The correlation of peak ground acceleration amplitude with seismic intensity and other physical

parameters. *Bulletin of the Seismological Society of America, 67,* 877–915.

Nemčok, M., Feyzullayev, A., Kadirov, A., Zeynalov, G., Allen, R., Christensen, C., et al. (2011). Neotectonics of the Caucasus and Kura valley, Azerbaijan. *Global Engineers and Technologist Review, 1*(1), 1–14.

Nilforoushan, F., Masson, F., Vernant, P., Vigny, C., Martinod, J., Abbassi, M., et al. (2003). GPS network monitors the Arabia-Eurasia collision deformation in Iran. *Journal of Geodesy, 77,* 411–422. https://doi.org/10.1007/s00190-003-0326-5.

Ordóñez, G. A. (2003). SHAKE2000: A computer program for the 1-D analysis of the geotechnical earthquake engineering problem.

Panza, G., Irikura, K., Kouteva-Guentcheva, M., Peresan, A., Wang, Z., & Saragoni, R. (Eds.). (2011). *Advanced seismic hazard assessment* (1st ed., Vol. 168, p. 752). Basel: Springer.

Panza, G., Romanelli, F., & Vaccari, F. (2001). Seismic wave propagation in laterally heterogeneous anelastic media: Theory and applications to seismic zonation. *Advances in Geophysics, 43,* 1–95.

Philip, H., Cisternas, A., Gvishiani, A., & Gorshkov, A. (1989). The Caucasus: An actual example of the initial stages of continental collision. *Tectonophysics, 161,* 1–21.

Reilinger, R. E., McClusky, S. C., Vernant, P., Lawrence, S., Ergintav, S., Cakmak, R., et al. (2006). GPS constraints on continental deformation in the Africa–Arabia–Eurasia continental collision zone and implications for the dynamics of plate interactions. *Journal of Geophysical Research, 111,* B5. https://doi.org/10.1029/2005jb004051.

Riznichenko, Yu V. (1965). From the activity of seismic sources to the intensity recurrence at the ground surface. *Izvestiya Akademii Nauk Sssr Fizika Zemli, 11,* 1–12. **(in Russian)**.

Scordilis, E. M. (2006). Empirical global relations converting Ms and mb to moment magnitude. *Journal of Seismology, 10,* 225–236.

Seed, H. B., Idriss, J. M., & Kiefer, F. M. (1969). Characteristics of Rock Motions during Earthquakes. *ASCE Journal of the Soil Mechanics and Foundations Division, 20,* 95.

Shebalin, N. (1961). Intensity, magnitude, and source depth of earthquakes. *Earthquakes in the USSR* (pp. 126–138). Moscow: USSR Academy of Sciences.

Telesca, L., Kadirov, F., Yetirmishli, G., Safarov, F., Babayev, G., & Ismaylova, S. (2017). Statistical analysis of the 2003–2016 seismicity of Azerbaijan and surrounding areas. *Journal of Seismology, 21,* 1467–1485. https://doi.org/10.1007/s10950-017-9677-x.

Telesca, L., Lovallo, M., Babayev, G., & Kadirov, F. (2013). Spectral and informational analysis of seismicity: An application to the 1996–2012 seismicity of Northern Caucasus–Azerbaijan part of Greater Caucasus–Kopet Dag Region. *Physica A Statistical Mechanics and Its Applications, 392,* 6064–6078. https://doi.org/10.1016/j.physa.2013.07.031.

Trifunac, M., & Brady, A. (1975). On the correlation of seismic intensity scales with the peaks of recorded strong ground motion. *Bulletin of the Seismological Society of America, 65,* 139–162.

Utsi, T. (1961). Ststistical study of occurrence of aftershocks. *Geophysical Magazine, 30,* 521–605.

Veber, M. V. (1904). *Recherches preliminaries sur le tremblement de terrea Chamakha, Comptes Rendue des Seances, Tome I* (pp. 238–241). St.-Petersbourg: Academie Imperiale des Sciences.

Wiemer, S., & Wyss, M. (2000). Minimum magnitude of completeness in earthquake catalogs: Examples from Alaska, the western United States, and Japan. *Bulletin of the Seismological Society of America, 90,* 859–869.

Developments Series No. 15, SEG Reference Publications, Society of Exploration Geophysics Reference Publications Program, Tulsa, Oklahoma-USA. Society of Exploration Geophysicists, American.

Kuliyev, F. T. (1986). *Otchet o seysmicheskom mikrorayonirovanii territorii Bolshogo Baku* (p. 56). Baku: Fond Instituta Geologii AN Azerb SSR.

Mammadli, T. Y. (2007). Weak seismicity of Azerbaijan territory and its relation with the contemporary geodynamics. Post-doctoral dissertation thesis, Baku, Azerbaijan, p. 350 **(original in Azerbaijani)**.

Yetirmishli, G. C., Mammadli, T. Y., & Kazimova, S. E. (2013). Features of seismicity of Azerbaijan part of the Greater Caucasus. *Journal of Georgian Geophysical Society, Issue (A), Physics of Solid Earth, 16a,* 55–60.